Available online at www.sciencedirect.com
ScienceDirect
Journal of Magnetic Resonance 182 (2006) 173–177
JMR Journal of Magnetic Resonance
www.elsevier.com/locate/jmr

Communication

Revisiting the initial rate approximation in kinetic NOE measurements

Haitao Hu *, Krish Krishnamurthy

Discovery Chemistry Research and Technologies, Lilly Research Laboratories, Eli Lilly and Company, Indianapolis, IN 46285, USA

Received 5 April 2006; revised 31 May 2006
Available online 27 June 2006

Abstract

The nuclear Overhauser effect (NOE) is undoubtedly one of the most useful tools in NMR spectroscopy and is widely used in solving structural and conformational problems of small organic molecules and macromolecular systems alike. In particular, measurement of the kinetics of the NOE, often facilitated by selective 1D NOE buildup experiments, can generate invaluable quantitative distance information for the molecule being investigated. In practice, analysis of such kinetic NOE data routinely assumes a first-order approximation of the initial buildup rate. However, often times such an approximation holds true only for the shortest mixing times. As shown by Macura and others, the linear range of the NOE buildup obtained from 2D NOESY and exchange experiments can be substantially extended by simply scaling the NOE cross-peaks against the corresponding diagonal peaks. In this note, we demonstrate through a detailed analysis that the same approach can be applied to the analysis of 1D NOE data obtained with the DPFGSE NOE pulse sequence, one of the most widely used selective 1D NOE experiments today. We show that this approach allows the inclusion of data points acquired with much longer mixing times in the analysis and thus considerably improves the accuracy of the measured cross-relaxation rates and internuclear distances, while considerably simplifying the data analysis. Similar results can be obtained for the rotating frame DPFGSE ROE experiment.

Keywords: DPFGSE NOE; DPFGSE ROE; Initial rate approximation; NOE buildup; Peak amplitude normalization for improved cross-relaxation; PANIC

1. Introduction

The nuclear Overhauser effect (NOE) is undoubtedly one of the most important discoveries in NMR spectroscopy [1]. Today it is widely used in solving structural and conformational problems of small organic molecules to macromolecular systems alike [2]. In particular, the kinetics of the NOE provides quantitative measurements of the internuclear distances involved, which are extremely valuable in the configurational and conformational analysis of small-to-medium sized organic molecules in solution [2]. Such measurements are often conducted with selective 1D kinetic NOE experiments [3–6], in which the cross-relaxation rates are extracted from the slopes of the respective NOE buildup curves, assuming a linear dependence of the NOE growth rate on τ_m, or the initial rate approximation. The corresponding internuclear distances are subsequently calculated from the cross-relaxation rates using some well-defined distances, such as that between the geminal protons of a methylene group. However, the initial rate approximation can cause large errors as the NOE grows, limiting the utility of the NOE buildup method to only the shortest mixing times.

Macura and others [7–10] have shown that, in the analysis of 2D NOESY and exchange experiments, the linearity of the initial buildup rate can be substantially extended by taking the ratio of the cross-peak to the diagonal peak, a technique we will refer to as peak amplitude normalization for improved cross-relaxation (PANIC) hereinafter for the sake of simplicity. Other benefits of the PANIC approach have also been discussed in the original work. However, their approach does not seem to have been widely adopted today for the analysis of 1D NOE data. Here, we

* Corresponding author. Fax: +1 317 433 4315.
E-mail address: hu_haitao@lilly.com (H. Hu).

1090-7807/$ - see front matter © 2006 Elsevier Inc. All rights reserved.
doi:10.1016/j.jmr.2006.06.009

demonstrate through a detailed analysis that the PANIC approach can be successfully applied to 1D NOE data obtained with the DPFGSE NOE pulse sequence [5,6], one of the most widely used selective 1D NOE experiments today. The PANIC approach allows the inclusion of data points acquired with much longer mixing times into the final analysis and thus considerably improves the accuracy of the measured cross-relaxation rates and internuclear distances.

2. Results and discussion

The DPFGSE NOE sequence is a transient NOE experiment whose excellent artifact suppression has allowed the detection of NOE enhancements as small as 0.02% [6]. Fig. 1 shows a slightly modified version used in this work [11], which has incorporated the recent advancement in zero-quantum suppression into the NOE mixing period [12]. In this experiment, the target spin is selectively retained by the DPFGSE sequence, which is subsequently aligned along either the $+z$ or $-z$ axis in alternate scans, resulting in a difference spectrum.

The kinetics of the NOE in the DPFGSE NOE experiment can be analyzed by explicitly solving the Solomon equations. For simplicity, consider a two spin system

$$\begin{aligned}\frac{dM_z^A}{dt} &= -R_A(M_z^A - M_0) - \sigma_{AB}(M_z^B - M_0)\\ \frac{dM_z^B}{dt} &= -R_B(M_z^B - M_0) - \sigma_{AB}(M_z^A - M_0),\end{aligned} \tag{1}$$

where M_0 is the equilibrium z magnetization for spins A and B (assumed to be identical), R_A and R_B are the auto-relaxation rate constants of spins A and B, and σ_{AB} is the cross-relaxation rate constant between spins A and B, respectively. Consider the case where spin B is selectively excited. The net magnetization of spin B at point a in Fig. 1 is given by κM_0, where the scaling factor $\kappa(0 \leqslant \kappa \leqslant 1)$ has been introduced to account for signal loss during the DPFGSE. At the beginning of the mixing time

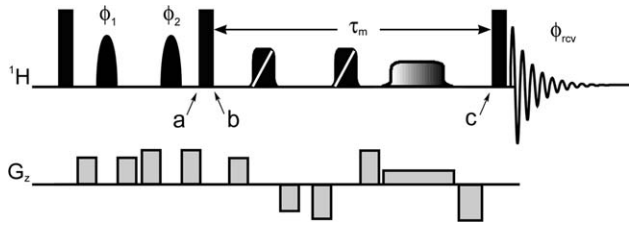

Fig. 1. Timing diagram of the modified DPFGSE NOE pulse sequence used in this work. Hard 90° pulses are represented by solid bars and selective 180° pulses by solid shaped icons. "Nulling" 180° pulses are denoted by the scored icons. Frequency-swept inversion pulses used for zero quantum suppression are indicated by the shaded icons. All pulses have phase x unless noted otherwise. All gradient pulses were applied along the z-axis without shaping. The basic phase cycle is $\phi_1 = x, y, -x, -y$; $\phi_2 = x$; $\phi_{rcv} = x, -x$. If desired, EXORCYCLE phase cycling can be independently applied to ϕ_1 and ϕ_2 to yield a 16-step phase cycle.

(point b in Fig. 1), spin B is either inverted ($M_z^B(t=0)/M_0 = -\kappa$) or aligned along the $+z$ axis ($M_z^B(t=0)/M_0 = +\kappa$) in alternate scans, resulting in either a spectrum with the desired NOE enhancement or a "reference" spectrum with no appreciable NOE enhancement at spin A. In both scans, we have $M_z^A(t=0)/M_0 = 0$. Explicitly solving the Solomon equations under these initial conditions yields the following results for spin A at the end of the mixing time (point c in Fig. 1),

$$\begin{aligned}M_z^A(\tau_m)/M_0 = &-\frac{(R_A - \lambda_2) + (1+\kappa)\sigma_{AB}}{\rho}e^{-\lambda_1 t}\\ &+\frac{(R_A - \lambda_1) + (1+\kappa)\sigma_{AB}}{\rho}e^{-\lambda_2 t} + 1,\end{aligned} \tag{2a}$$

$$\begin{aligned}M_z^A(\tau_m)_{ref}/M_0 = &-\frac{(R_A - \lambda_2) + (1-\kappa)\sigma_{AB}}{\rho}e^{-\lambda_1 t}\\ &+\frac{(R_A - \lambda_1) + (1-\kappa)\sigma_{AB}}{\rho}e^{-\lambda_2 t} + 1,\end{aligned} \tag{2b}$$

where $\rho = \sqrt{(R_A - R_B)^2 + 4\sigma_{AB}^2}$, $\lambda_1 = (R_A + R_B + \rho)/2$, and $\lambda_2 = (R_A + R_B - \rho)/2$. The NOE enhancement at spin A expressed as a fraction of the equilibrium magnetization is then by definition given by the difference between Eqs. (2a) and (2b),

$$\begin{aligned}\eta_{NOE}(\tau_m) &= \frac{M_z^A(\tau_m) - M_z^A(\tau_m)_{ref}}{M_0}\\ &= \frac{2\kappa\sigma_{AB}}{\rho}(e^{-\lambda_2\tau_m} - e^{-\lambda_1\tau_m}).\end{aligned} \tag{3}$$

Note that in the above analysis the broadband 180° pulses (scored icons in Fig. 1) during the NOE mixing time have been neglected, as they do not affect the net outcome of the NOE buildup [6]. The effect of the z-filter is not entirely clear, other than the fact that it results in a slightly lengthened mixing time compared to the nominal value. In practice, this does not seem to cause any noticeable problems. If desired, however, its effect can be largely removed by subtracting a reference spectrum recorded with "zero" mixing time for the same target spin, yielding a double difference spectrum [13]. Additional advantages of the double difference spectrum include its improved suppression of artifacts due to spin state mixing [13] and its dramatically reduced target peak, allowing more accurate quantitation of NOE peaks close to the target resonance.

In the initial rate regime, the exponential terms in Eq. (3) can be substituted with their Taylor series. Discarding all 2nd and higher order terms in τ_m, we obtain

$$\eta_{NOE}(\tau_m) \approx 2\kappa\sigma_{AB}\tau_m. \tag{4}$$

The value of κ can be determined by comparing the integral of the target resonance in the 1D DPFGSE NOE experiment acquired with zero mixing time to that in a simple 1D pulse-acquire experiment [6], thus allowing the cross-relaxation rate σ_{AB} to be extracted from the NOE buildup by a simple linear regression. This is in fact the widely accepted practice today. As shown in Fig. 2a, however, even for a

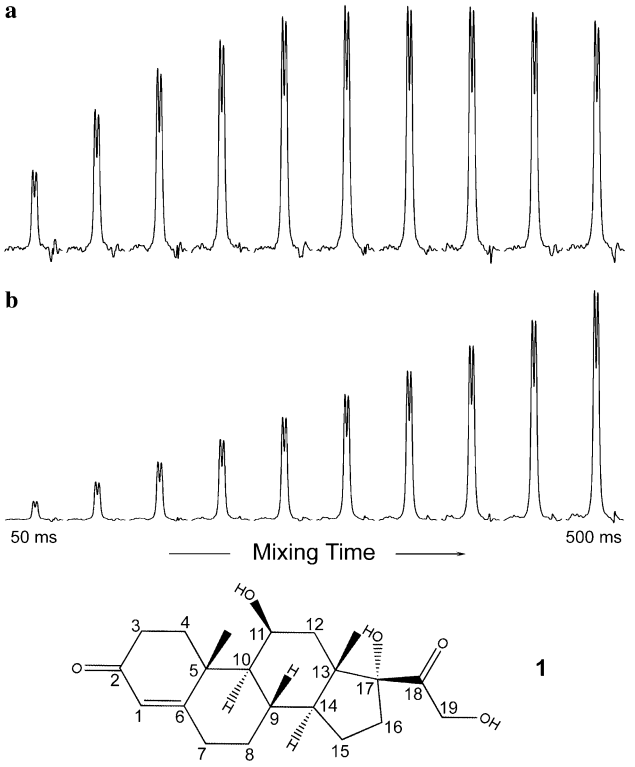

Fig. 2. NOE buildup curves of H_{10} while selectively exciting H_{4axial} of cortisol (**1**) in DMSO-d_6: (a) the "raw" NOE buildup curve; (b) the NOE buildup curve obtained with PANIC. The NOE mixing time (τ_m) was systematically increased from 50 to 500 ms in 50 ms steps. All spectra were collected with 512 transients on a 400 MHz Varian UnityInova spectrometer equipped with a 5 mm ^{1}H{X} indirect detection probe and z-gradient accessory. The recycling delay was set to 5 s. Each FID was acquired with 4096 points over a spectral width of 4000 Hz and zero-filled to 16,384 points before Fourier transformation using a 4 Hz line broadening window function.

small molecule the size of cortisol in DMSO, the NOE buildup curve can start to deviate significantly from the initial rate approximation at rather moderate mixing times (~250 ms). As a result, the linear regression is forced to be limited to only those data points acquired with the shortest mixing times and thus the lowest signal-to-noise ratios. This issue is exacerbated for the measurement of medium-to-long range distances, for which the NOE enhancements are inevitably much weaker, even though such distances are clearly more valuable from a structural analysis point of view.

The above example shows that the initial rate approximation can be rather poor for even moderate mixing times. A much improved approximation to Eq. (3) is achieved by retaining all 2nd order terms in the Taylor series as well,

$$\eta_{\mathrm{NOE}}(\tau_m) \approx 2\kappa\sigma_{\mathrm{AB}}\tau_m(1 - R\tau_m), \tag{5}$$

where $R_{\mathrm{A}} \approx R_{\mathrm{B}} = R$ has been assumed. Eq. (5) indicates that the nonlinearity of the NOE buildup at relatively short-to-moderate mixing times is largely due to external relaxation. However, such deviation from the initial rate approximation is often incorrectly attributed to spin diffusion (for a multi-spin system, of course), which is generally negligible for small-to-medium sized molecules under the conditions considered here. While it may be possible to fit Eq. (5) to a 2nd order polynomial, this is undesirable for several reasons. First, a non-linear least-squares fit is less stable, especially as the number of parameters to be fitted increases. Second, in theory, a linear regression requires only two data points. In the special case where the intercept is known to be zero, a single point suffices. In contrast, a non-linear least-squares fit demands a much larger number of data points in order to achieve the desired accuracy. Instead, we demonstrate that the PANIC approach proposed by Macura et al. [7–10] largely restores the linear dependence of the NOE enhancement on τ_m for significantly longer mixing times using the very same dataset.

The key to the solution is the target spin, whose fate we have ignored so far. Explicitly solving the Solomon equations yields

$$\begin{aligned}\eta_{\mathrm{target}}(\tau_m) &= \frac{M_z^{\mathrm{B}}(\tau_m) - M_z^{\mathrm{B}}(\tau_m)_{\mathrm{ref}}}{M_0} \\ &= \frac{2\kappa}{\rho}\{R_{\mathrm{B}}(\mathrm{e}^{-\lambda_2\tau_m} - \mathrm{e}^{-\lambda_1\tau_m}) + (\lambda_2\mathrm{e}^{-\lambda_1\tau_m} - \lambda_1\mathrm{e}^{-\lambda_2\tau_m})\}.\end{aligned} \tag{6}$$

Note that

$$\eta_{\mathrm{target}}(\tau_m = 0) = \frac{2\kappa}{\rho}(\lambda_2 - \lambda_1) = -2\kappa \tag{7}$$

as discussed earlier. Again assuming $R_{\mathrm{A}} \approx R_{\mathrm{B}} = R$, we obtain

$$\begin{aligned}\rho &= \sqrt{(R_{\mathrm{A}} - R_{\mathrm{B}})^2 + 4\sigma_{\mathrm{AB}}^2} \approx 2\sigma_{\mathrm{AB}} \\ \lambda_1 &= (R_{\mathrm{A}} + R_{\mathrm{B}} + \rho)/2 \approx R + \sigma_{\mathrm{AB}} \\ \lambda_2 &= (R_{\mathrm{A}} + R_{\mathrm{B}} - \rho)/2 \approx R - \sigma_{\mathrm{AB}}\end{aligned} \tag{8}$$

Eq. (6) then simplifies to

$$\begin{aligned}\eta_{\mathrm{target}}(\tau_m) &= \frac{M_z^{\mathrm{B}}(\tau_m) - M_z^{\mathrm{B}}(\tau_m)_{\mathrm{ref}}}{M_0} \\ &\approx -\frac{2\kappa\sigma_{\mathrm{AB}}}{\rho}(\mathrm{e}^{-\lambda_1\tau_m} + \mathrm{e}^{-\lambda_2\tau_m}).\end{aligned} \tag{9}$$

Dividing the NOE enhancement (Eq. (3)) by the target magnetization (Eq. (9)), we find

$$\begin{aligned}\zeta_{\mathrm{NOE}}(\tau_m) &= \left|\frac{\eta_{\mathrm{NOE}}(\tau_m)}{\eta_{\mathrm{target}}(\tau_m)}\right| = \left|\frac{M_z^{\mathrm{A}}(\tau_m) - M_z^{\mathrm{A}}(\tau_m)_{\mathrm{ref}}}{M_z^{\mathrm{B}}(\tau_m) - M_z^{\mathrm{B}}(\tau_m)_{\mathrm{ref}}}\right| \\ &\approx \frac{\mathrm{e}^{-\lambda_2\tau_m} - \mathrm{e}^{-\lambda_1\tau_m}}{\mathrm{e}^{-\lambda_2\tau_m} + \mathrm{e}^{-\lambda_1\tau_m}} \approx \frac{\mathrm{e}^{-R\tau_m}(\mathrm{e}^{\sigma_{\mathrm{AB}}\tau_m} - \mathrm{e}^{-\sigma_{\mathrm{AB}}\tau_m})}{\mathrm{e}^{-R\tau_m}(\mathrm{e}^{\sigma_{\mathrm{AB}}\tau_m} + \mathrm{e}^{-\sigma_{\mathrm{AB}}\tau_m})} \\ &= \tanh(\sigma_{\mathrm{AB}}\tau_m),\end{aligned} \tag{10}$$

where $\zeta_{\mathrm{NOE}}(\tau_m)$ is the NOE enhancement normalized against the target signal within the *same* spectrum, instead of its equilibrium value. Eq. (10) reveals that the effect of external relaxation is completely cancelled out in this approach. Replacing the hyperbolic tangent function in Eq. (10) with its Taylor series, we obtain

$$\begin{aligned}\zeta_{\mathrm{NOE}}(\tau_m) &\approx \tanh(\sigma_{\mathrm{AB}}\tau_m)\\ &= \sigma_{\mathrm{AB}}\tau_m - \frac{1}{3}(\sigma_{\mathrm{AB}}\tau_m)^3 + \frac{2}{15}(\sigma_{\mathrm{AB}}\tau_m)^5 + \cdots\\ &\approx \sigma_{\mathrm{AB}}\tau_m, \end{aligned} \tag{11}$$

where all 3rd and higher order terms in τ_m have been discarded.

Evidently, Eq. (11) should be significantly more accurate than Eq. (4), since it is a 2nd order approximation in τ_m while the latter amounts to a 1st order approximation. Yet the desired linear dependence of the NOE enhancement on τ_m is better approximated in the PANIC approach because of the vanishing 2nd order term in Eq. (11). In other words, with the PANIC approach, the NOE buildup curve should remain linear for much longer mixing times. In addition, knowledge of the scaling factor κ is no longer necessary in the PANIC approach, eliminating the need to acquire a 1D DPFGSE NOE spectrum with zero mixing time for each individual target. Neither is it necessary to normalize the "cross-peak" intensities against the equilibrium magnetization as in the conventional approach, which should become evident by comparing the definition of $\zeta_{\mathrm{NOE}}(\tau_m)$ (Eq. (10)) vs. that of $\eta_{\mathrm{NOE}}(\tau_m)$ (Eq. (3)). Since in the PANIC approach both the NOE and the target resonances are from the same spectrum, potential errors caused by variations from experiment to experiment are also minimized [7,8].

Eq. (11) is strictly true only if $R_{\mathrm{A}} = R_{\mathrm{B}}$. If this condition is not met, then the PANIC approach may not completely eliminate the 2nd order term in τ_m. In the extreme case where $R_{\mathrm{A}} \gg R_{\mathrm{B}}$, we obtain $\rho \approx R_{\mathrm{A}} - R_{\mathrm{B}}$, it can be shown that Eq. (11) transforms to

$$\begin{aligned}\zeta_{\mathrm{NOE}}(\tau_m) &\approx \frac{\sigma_{\mathrm{AB}}}{R_{\mathrm{A}} - R_{\mathrm{B}}}(1 - \mathrm{e}^{-(R_{\mathrm{A}} - R_{\mathrm{B}})\tau_m})\\ &= \sigma_{\mathrm{AB}}\tau_m - \frac{1}{2}\sigma_{\mathrm{AB}}(R_{\mathrm{A}} - R_{\mathrm{B}})\tau_m^2 + \frac{1}{6}\sigma_{\mathrm{AB}}(R_{\mathrm{A}} - R_{\mathrm{B}})^2\tau_m^3 + \cdots \end{aligned} \tag{12}$$

Clearly, the 2nd order term in τ_m is no longer negligible. In practice, however, this is rarely the case and the PANIC approach does a very reasonable job in minimizing the 2nd order deviation.

The above observation can be easily verified experimentally. Fig. 2b shows the NOE buildup curve obtained with the PANIC approach. It uses the very same dataset as that used in Fig. 2a, except that the intensity of the target resonance (not shown) in each spectrum has been normalized to have the same height as that in the zero mixing time spectrum. This in effect displays $\zeta_{\mathrm{NOE}}(\tau_m)$ scaled by a constant, $\eta_{\mathrm{target}}(\tau_m = 0)M_0$. The dramatic improvement in the linearity of the NOE buildup allows all data points, particularly those with longer mixing times and thus the best signal-to-noise, to be included in the linear regression analysis, thereby significantly improving the accuracy of the cross-relaxation rate constants so obtained. As an example, the correlation coefficient of the linear regression analysis for the corresponding dataset using the peak intensities in Fig. 2b is greater than 0.99, typical of our data analyzed in this fashion.

Alternatively, for a given amount of total experiment time, fewer data points with higher signal-to-noise ratios (by acquiring more transients) can be used in the linear regression analysis without sacrificing accuracy. This is particularly relevant for the accurate measurement of medium-to-long range distances, where excellent signal-to-noise is a must. If desired, these fewer data points can even be skewed towards longer mixing times to give the best signal-to-noise. It is noteworthy that even though the PANIC approach appears to extend the linear range of the NOE buildup well beyond the cross-peak maximum in the conventional approach, the mixing times used in this work typically do not exceed 500 ms in order to keep spin diffusion to a minimum.

Interestingly, the apparent NOE buildup rate in Fig. 2a is about twice that of Fig. 2b. A comparison of Eq. (4) to Eq. (11) reveals that this is exactly as predicted by the above analysis. Therefore the cross-relaxation rates obtained by the PANIC approach and the conventional method using only the linear portion of the NOE buildup should be identical.

For medium sized molecules, the NOE cross-relaxation rate can be vanishingly small, in which case the rotating frame Overhauser effect (ROE) can be measured [14,15]. A similar analysis has been carried out for the 1D DPFGSE ROE experiment (results not shown). Not surprisingly, almost identical results to those for the NOE buildup are obtained.

3. Conclusions

In summary, we have shown through a detailed analysis that the PANIC approach proposed by Macura et al. for the analysis of 2D NOESY and exchange data fully applies to kinetic NOE and ROE data obtained with the widely used selective 1D DPFGSE NOE experiment and its rotating frame counterpart. This allows those data points significantly beyond the initial linear regime, which otherwise have the highest signal-to-noise ratios, to be included in the analysis, thereby improving the accuracy of the measured cross-relaxation rates. The success of this approach lies in that it utilizes the target resonance within the same spectrum to cancel out the nonlinear component in the NOE buildup curve, which is largely caused by external relaxation for moderate mixing times. The cross-relaxation rate can then be extracted from the resultant dataset by a straightforward linear regression analysis just as in the conventional method. In addition, the PANIC approach does not require knowledge of the scaling factor and eliminates the need for normalizing against the equilibrium magnetization, further simplifying the data analysis. While the above results are demonstrated for a two spin system, they can be easily extended to multi-spin systems.

References

[1] J.H. Noggle, R.E. Schirmer, The Nuclear Overhauser Effect: Chemical Applications, Academic Press, New York, 1971.

[2] D. Neuhaus, M.P. Williamson, The Nuclear Overhauser Effect in Structural and Conformational Analysis, Second ed., Wiley-VCH, New York, 2000.

[3] H. Kessler, H. Oschkinat, C. Griesinger, W. Bermel, Transformation of homonuclear two-dimensional NMR techniques into one-dimensional techniques using Gaussian pulses, J. Magn. Reson 70 (1986) 106–133.

[4] J. Stonehouse, P. Adell, J. Keeler, A.J. Shaka, Ultrahigh-quality NOE spectra, J. Am. Chem. Soc. 116 (1994) 6037–6038.

[5] K. Stott, J. Stonehouse, J. Keeler, T.-L. Hwang, A.J. Shaka, Excitation sculpting in high-resolution nuclear magnetic resonance spectroscopy: application to selective NOE experiments, J. Am. Chem. Soc. 117 (1995) 4199–4200.

[6] K. Stott, J. Keeler, Q.N. Van, A.J. Shaka, One-dimensional NOE experiments using pulsed field gradients, J. Magn. Reson. 125 (1997) 302–324.

[7] S. Macura, B.T. Farmer II, L.R. Brown, An improved method for the determination of cross-relaxation rates from NOE data, J. Magn. Reson. 70 (1986) 493–499.

[8] G. Esposito, A. Pastore, An alternative method for distance evaluation from NOESY spectra, J. Magn. Reson. 76 (1988) 331–336.

[9] G. Bodenhausen, R.R. Ernst, Direct determination of rate constants of slow dynamic process by two-dimensional "accordion" spectroscopy in nuclear magnetic resonance, J. Am. Chem. Soc. 104 (1982) 1304–1309.

[10] N. Juranić, Z. Zolnai, S. Macura, Two-dimensional exchange spectroscopy revisited: accounting for the number of participating spins, J. Serb. Chem. Soc. 65 (2000) 285–301.

[11] H. Hu, S.A. Bradley, K. Krishnamurthy, Extending the limits of the selective 1D NOESY experiment with an improved selective TOCSY edited preparation function, J. Magn. Reson. 171 (2004) 201–206.

[12] M.J. Thrippleton, J. Keeler, Elimination of zero-quantum interference in two-dimensional NMR spectra, Angew. Chem. Int. Ed. Engl. 42 (2003) 3938–3941.

[13] K.E. Cano, M.J. Thrippleton, J. Keeler, A.J. Shaka, Cascaded *z*-filters for efficient single-scan suppression of zero-quantum coherence, J. Magn. Reson. 167 (2004) 291–297.

[14] A.A. Bothner-By, R.L. Stephens, J.-M. Lee, C.D. Warren, R.W. Jeanloz, Structure determination of a tetrasaccharide: transient nuclear Overhauser effects in the rotating frame, J. Am. Chem. Soc. 106 (1984) 811–813.

[15] A. Bax, D.G. Davis, Practical aspects of two-dimensional transverse NOE spectroscopy, J. Magn. Reson. 63 (1985) 207–213.